

Integrated Heat Transport Simulation of Multi-Ion-Species Plasma in LHD^{*)}

Akira SAKAI, Sadayoshi MURAKAMI, Hiroyuki YAMAGUCHI, Arimitsu WAKASA and Atsushi FUKUYAMA

Department of Nuclear Engineering, Kyoto University, Kyoto 615-8540, Japan

(Received 10 December 2013 / Accepted 14 April 2014)

In this study, we have investigated the heat transport of multi-ion species plasma by modifying and improving the integrated simulation code TASK3D in LHD. The impurities in the electron and hydrogen plasmas were assumed to be helium and carbon. Turbulent transport is assumed to be independent of the impurity density ratio. The ion temperature, which is higher for carbon than that for helium, increases linearly as the impurity density ratio increases. The increment of the ion temperature is due to the decrease in the effective neoclassical heat transport and the ion density. The ion temperature increment is higher in the case of lower density.

© 2014 The Japan Society of Plasma Science and Nuclear Fusion Research

Keywords: integrated simulation, heat transport, multi-ion-species plasma

DOI: 10.1585/pfr.9.3403124

1. Introduction

TASK3D [1] is an integrated transport code for helical plasmas and was developed based on the TASK code in a collaboration between Kyoto University and NIFS. Using the TASK3D code, we performed: (i) self-consistent calculations of the heat transport and the distribution of heating power in LHD experimental plasmas (assuming steady state) [2]. and (ii) simulations of the plasma development with time by using gas puff control and power modulation [3]. These analyses have shown the good capability of the integrated simulation by the TASK3D.

In a previous study, we assumed that the plasma consists of a single-ion species. However, in reality, there are many impurity sources, such as the surface of plasma-facing components and the diverter plate. In addition, we intentionally injected impurities to the core plasma in order to control the density and plasma heating. For example, in the high-Ti experiment of LHD [4], a carbon pellet and helium gas puff is injected into the plasma in order to control the density profile and increase the ion temperature. In this experiment, a rapid increase was observed in the ion temperature after the injection of carbon pellet. The improvement in turbulent transport plays an important role in the temperature increase; however, additional improvements are anticipated due to the injection of impurities. In the experiments, when assuming one-component plasma, the correct result could not be obtained because the impurity density ratio was very large. Therefore, we require an integrated simulation code capable of analyzing the heat transport of multi-ion species plasma.

In this study, we modify and improve the integrated

simulation code TASK3D to treat multi-ion species plasma and study the effect of impurities on the heat transport in the LHD plasma. We consider two kinds of impurities, such as helium and carbon, in the electron and hydrogen plasma. We also assume that the turbulent transport is independent of the impurity ratio. We then study the effect of the change of the neoclassical transport and ion density on the heat transport. We show the change in the heat transport while increasing the impurity ratio and clarify the effect of impurities on the heat transport in the LHD plasma.

2. Simulation Model

Physical phenomena in fusion plasma have a wide range in time and space, and the dominant phenomena are different in each regime. Thus, simulating fusion plasma by using a single model is difficult. TASK3D is an integrated simulation code in which each module describes a physical phenomenon and simulates fusion plasmas using multiple models. To simulate heat transport, we use five modules such as VMEC [5], FIT3D [6], DGN/LHD [7], ER, and TR in TASK3D.

- (a) VMEC is a three-dimensional variational moment equilibrium code, which evaluates the MHD equilibrium in three-dimensional magnetic configuration.
- (b) FIT3D evaluates the radial profile of the NBI power deposition, beam-driven current, and beam density and pressure. There are three steps in the FIT3D calculations.
 - First, the beam ion birth points are calculated by injecting the beam particle from the ion source using Monte Carlo methods.
 - Second, the radial redistribution of beam ions

author's e-mail: sakai@p-grp.nucleng.kyoto-u.ac.jp

^{*)} This article is based on the presentation at the 23rd International Toki Conference (ITC23).

due to prompt orbit effects is evaluated following the test particle orbit in the Boozer coordinates.

- Finally, radial profiles of heat deposition are evaluated by solving the Fokker—Planck equation in the $(v_{\parallel}, v_{\perp})$ space.

- (c) DGN/LHD is the neoclassical transport database for LHD plasma. The thermal radial transport coefficients are evaluated by using the convolution of the monoenergetic diffusion coefficient with Maxwellian distribution. The monoenergetic diffusion coefficients are obtained by using the normalized diffusion coefficient database based on the neural network method.
- (d) ER calculates the radial electric field, which is critical to the heat transport of plasma. The radial electric field equation of the ER module is expressed by

$$\frac{\partial E_r}{\partial t} = -\frac{e}{\epsilon_{\perp}} \sum_j Z_j \Gamma_j^{\text{NC}} + \frac{1}{r} \frac{\partial}{\partial r} \left(\sum_j Z_j D_{E_r} \frac{\partial E_r}{\partial r} \right), \quad (1)$$

where D_E is the radial diffusion coefficient for the radial electric field and ϵ_{\perp} is the perpendicular dielectric coefficient [8]. ϵ_{\perp} is given as follows,

$$\epsilon_{\perp} = \epsilon_0 \left(\left(\frac{c^2}{v_A^2} \right) + 1 \right) (1 + 2q^2), \quad (2)$$

where ϵ_0 is the dielectric constant in vacuum, c is the speed of light, v_A is the velocity of the Alfvén wave and q is the safety factor. The factor $(1 + 2q^2)$ is added to introduce the toroidal effect.

To calculate E_r , we assume that D_E is constant and fixed in space and time. Figure 1 shows the radial profile of E_r for $D_E = 0.0, 3.0, 5.0$ and 10.0 [m²/s]. Boundary conditions are set at $E_r(r/a = 0) = 0$ [kV/m] and $E_r(r/a = 1) = 5$ [kV/m]. A small increase can be observed in E_r as D_E increases, but only in the region $r/a > 0.9$. Thus, we assume $D_E = 5$ [m²/s], which is based on the neoclassical heat transport, even if details regarding D_E are unknown.

- (e) TR calculates the radial transport of plasma by solving the diffusive equation given as follows,

$$\frac{\partial}{\partial t} \left(\frac{3}{2} n_s T_s \right) = -\frac{1}{V'} \frac{\partial}{\partial \rho} \left(V' \langle |\nabla \rho| \rangle n_s \left(V_{K_s} + \frac{3}{2} V_s \right) - V' \langle |\nabla \rho|^2 \rangle \left(\frac{3}{2} D_s T_s \frac{\partial n_s}{\partial \rho} + n_s \chi_s \frac{\partial T_s}{\partial \rho} \right) \right) + P_s,$$

where D_s is the particle diffusion coefficient, χ_s is the thermal conductivity, V_s is the particle pinch velocity, and V_{K_s} is the heat pinch velocity. Neoclassical components of D_s , V_s , V_{K_s} and χ_s are determined by DGN/LHD and we assume that the turbulence components of D_s , V_s and V_{K_s} are zero.

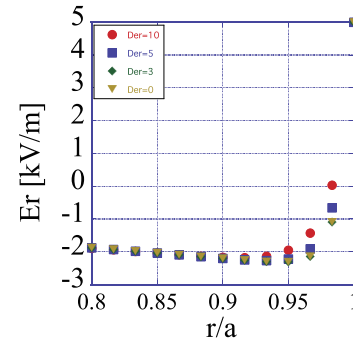


Fig. 1 Radial profile of the radial electric field with four different viscosity values, $D_E = 0.0, 3.0, 5.0, 10.0$ [m²/s].

We assume $\chi_s = \chi_s^{\text{NC}} + \chi_s^{\text{TB}}$, where χ_s^{NC} and χ_s^{TB} are the neoclassical and turbulence conductivities, respectively. For the turbulence component we apply the gyro-bohm model for electron and the gyro-bohm+gradTi model for

$$\chi_e^{\text{TB}} = C_e \left(\frac{T_e}{eB} \right) \left(\frac{\rho_e}{L} \right), \quad (3)$$

$$\chi_i^{\text{TB}} = C_i \left(\frac{T_i}{eB} \right) \left(\frac{\rho_i}{L} \right) \left(\frac{aT'_{\text{ave}}}{T_{\text{ave}}} \right), \quad (4)$$

where, $T_{\text{ave}} = (T_e + T_{i(\text{bulk})})/2$, ρ_e , ρ_i , B , and L are the average temperatures of the electron and bulk ions, the Larmor radius of the electron, the Larmor radius of the ion, the magnetic field strength, and the minor radius, respectively. The effect of multi-ion species on the turbulence heat transport remains unknown. Thus, in this study, we simply assume a heat transport model for the electron and proton plasma. Based on the previous study, we used the constant factors $C_e = 25$, $C_i = 9.07$ [2].

3. Simulation Results

To clarify the impurity density dependency of heat transport, we study the change in temperature, the radial electric field, and the heat conductivity as a function of the impurity density ratio. Note that in our model, the radial electric field is only related to the neoclassical thermal conductivity. We assume the magnetic field configuration of LHD as $R_{\text{ax}} = 3.6$ [m] and set the central magnetic field strength as $B_0 = 2.75$ [T].

Now, as shown in Table 1 we consider five NBI beam system in LHD i.e., three tangential and two perpendicular injection systems. We calculate each power deposition of the NBI beam system and sum up the total power. In FIT3D, the multi-energy component of the beam injection energy is considered in the perpendicular injection (positive ion source injector) case. Because FIT3D can only evaluate the heat deposition in single-ion species plasma, we assume the following model for multi-ion deposition

Table 1 Parameters of the NBI heating injectors #1 to #5 in the LHD.

| | beam energy [keV] | power [MW] | direction |
|----|-------------------|------------|---------------|
| #1 | 192.0 keV | 6.06 MW | tangential |
| #2 | 177.6 keV | 4.41 MW | tangential |
| #3 | 179.3 keV | 4.71 MW | tangential |
| #4 | 39.0 keV | 5.32 MW | perpendicular |
| #5 | 42.2 keV | 5.71 MW | perpendicular |

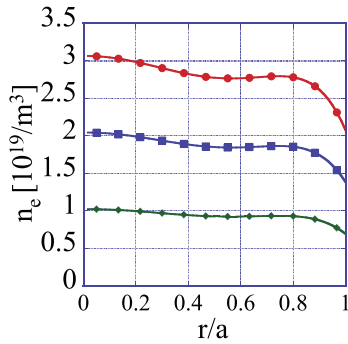

 Fig. 2 Electron density profiles of $n(r/a = 0) = 3.06 \times 10^{19}$, 2.04×10^{19} , $1.02 \times 10^{19} / \text{m}^3$ cases.

Table 2 Assumed impurity ratio in the (e,H,He) plasma.

| η_{He} | ξ_{He} |
|--------------------|-------------------|
| 14% | 25% |
| 33% | 50% |
| 60% | 75% |
| 78% | 88% |
| 85% | 92% |

Table 3 Assumed impurity ratio in the (e,H,C) plasma.

| η_{C} | ξ_{C} |
|-------------------|------------------|
| 5.3% | 25% |
| 14% | 50% |
| 33% | 75% |
| 54% | 88% |
| 65% | 92% |

profiles.

$$P_e = P_e^{\text{FIT3D}}, \quad (5)$$

$$P_s = \frac{n_s}{\sum_j^{\text{ion}} n_j} P_i^{\text{FIT3D}}, \quad (6)$$

where P_e^{FIT3D} and P_i^{FIT3D} are the power depositions of the electron and respectively calculated by FIT3D. n_j is the number density of each ion.

The assumed electron density profiles are shown in Fig. 2 and the hydrogen and impurity densities are given by

$$n_e = \sum_j^{\text{ion}} Z_j n_j, \quad (7)$$

$$\eta_s = \frac{n_s}{\sum_j^{\text{ion}} n_j}, \quad (8)$$

$$\xi_s = \frac{Z_s n_s}{\sum_j^{\text{ion}} Z_j n_j}. \quad (9)$$

We, first, consider the case $n_{\text{center}} = 3.06 \times 10^{19} / \text{m}^3$, and the impurity ratio of helium and carbon are varied according

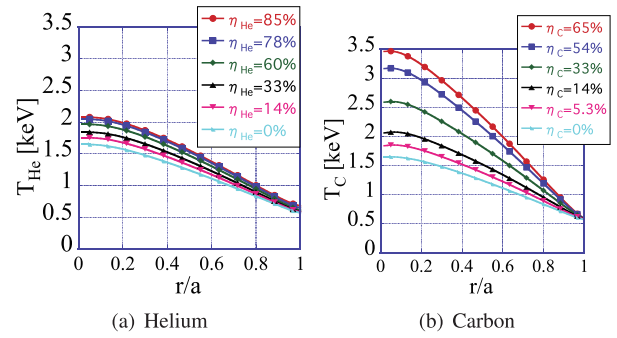


Fig. 3 Radial profile of ion temperature changing the impurity density ratio in the helium and carbon impurity cases.

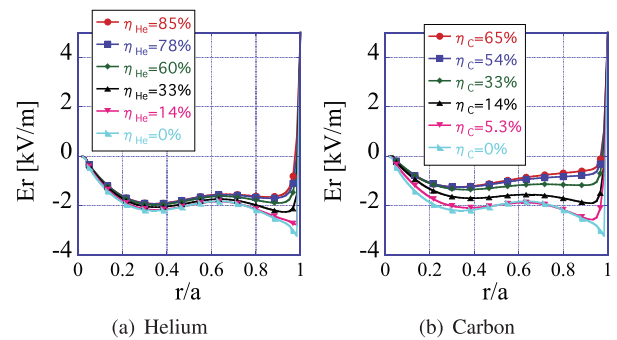


Fig. 4 Radial profile of radial electric field changing the impurity density ratio in the helium and carbon impurity cases.

to Tables 2 and 3. Next, we study the effect of the impurity ion ratio on the heat transport by changing the electron density as $n_{\text{center}} = 3.06 \times 10^{19}$, 2.04×10^{19} , $1.02 \times 10^{19} / \text{m}^3$.

Figure 3 shows the impurity temperature as a function of the impurity density ratio for helium and carbon. The impurity temperature increases as the impurity density ratio increases, and the increment is about 5.5 times larger for carbon. However, the electron temperature is almost independent of the impurity density ratio.

The radial electric field as a function of the impurity density ratio is shown in Fig. 4. The radial electric field shows the neoclassical ion root solution in most of the regions of plasma and only positive E_r in the edge region due to the boundary condition ($E_r > 0$ at the outside of LCFS). The magnitude of the radial electric field decreases as the impurity density ratio increases, especially at the edge of the plasma. For (e,H,He) plasma, the radial electric field does not vary in the $0.6 < r/a$ region; however, varies in almost all other regions for (e, H, C) plasma.

Next we show the effect of the impurity density ratio on the neoclassical transport. To analyze the neoclassical thermal conductivity, we define the effective neoclassical thermal conductivity as $\chi_{\text{eff}}^{\text{NC}} = \sum_j \chi_j^{\text{NC}} n_j / \sum_j n_j$ and divide the conductivity by the temperature dependence of the gyro-Bohm scaling, $T^{3/2}$. Figure 5 shows the radial profile of the effective neoclassical heat conductivity as a function of the impurity density ratio. A clear improvement can be

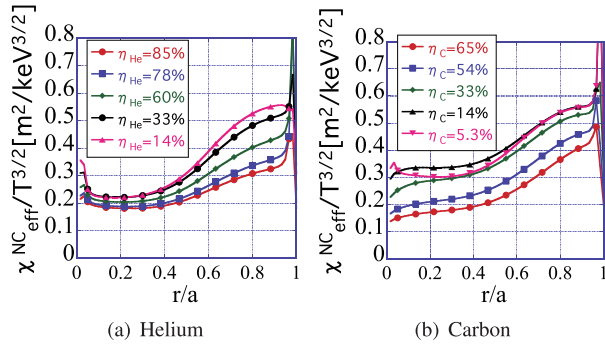


Fig. 5 Radial profile of effective thermal conductivity changing the impurity density ratio in the helium and carbon impurity cases.

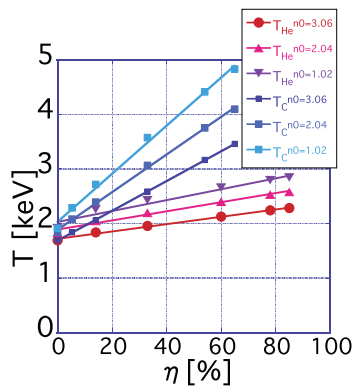


Fig. 6 Plots of the ion temperature at $r/a = 0$ as a function of the impurity density ratio in the different electron densities.

observed in the effective neoclassical transport in both the cases, and the improvement is larger for carbon.

Next, we study the impurity effect on the ion temperature by varying the total electron density. We consider the two additional lower electron density cases ($n_{r/a=0} = 2.06 \times 10^{19}, 1.02 \times 10^{19} / \text{m}^3$) shown in Fig. 2 and compare them with the obtained results. We observe that the heat deposition decreases as the electron density decreases because of the increase in the shine-through loss of the beam ions.

Figure 6 shows the change in the impurity temperature as a function of the impurity density ratio for three different density cases. The impurity ion temperature increases

linearly with increasing impurity density ratio in all density cases. In addition, the ion temperature increment is larger in the lower density cases. This is because the neoclassical transport increases in the lower density, and thus the improvement in the effective neoclassical transport due to impurity ions is more effective in the lower density case.

4. Conclusions

We modified and improved the integrated simulation code TASK3D to treat multi-ion component plasma and investigated the heat transport of multi-ion species plasma in LHD. We assumed helium and carbon impurities in the hydrogen plasma as (e, H, He) and (e, H, C). A typical density profile for the LHD experimental plasma is assumed and the heating profiles of the NBI heating system are evaluated by using the FIT3D module. In this study, we used the same heat deposition profile to clarify the multi-ion species effect on the heat transport. We have also studied the effect of multi-ion species on the NBI heating deposition, which is published elsewhere [9].

We determined that the ion temperature increases as the impurity density ratio increases for both the impurities, and that the temperature increase rate is higher for carbon. The temperature increases due to the decrease in the effective neoclassical heat transport and the ion density. Also, the increase in ion temperature becomes large in the case of lower electron density because of the larger contribution of the neoclassical transport in the lower density.

The results suggest that the carbon pellet injection plays a role in the reduction of the effective neoclassical transport, the decrease in the ion density, and the ion temperature increase in the high-Ti plasma of LHD.

- [1] M. Sato *et al.*, Plasma Fusion Res. **3**, S1063 (2008).
- [2] A. Wakasa *et al.*, Proc. 39th EPS Conf. and 16th Int. Cong. Plasma Phys., 2012, P2.028.
- [3] H. Yamaguchi *et al.*, JPS Conf. Proc (2014) in press.
- [4] H. Takahashi *et al.*, Nucl. Fusion **53**, 073034 (2013).
- [5] S.P. Hirshman, W.I. van Rij and P. Merkel, Comput. Phys. Commun. **43**, 143 (1986).
- [6] S. Murakami *et al.*, Trans. Fusion Technol. **27**, 256 (1995).
- [7] A. Wakasa *et al.*, Jpn. J. Appl. Phys. **46**, 1157 (2007).
- [8] S. Toda *et al.*, Plasma Fusion Res. SERIES **4**, 466 (2001).
- [9] H. Yamaguchi *et al.*, submitted to Plasma Fusion Res.